

Magnetohydrodynamic Simulation of the Radial Evolution and Stream Structure of Solar-Wind Turbulence

D. Aaron Roberts, Sanjoy Ghosh, and Melvyn L. Goldstein

Laboratory for Extraterrestrial Physics, NASA Goddard Space Flight Center, Greenbelt, Maryland 20771

William H. Matthaeus

Bartol Research Institute, University of Delaware, Newark, Delaware 19716

(Received 16 September 1991)

We present a unified interpretation of observations of interplanetary fluctuations in terms of nearly incompressible magnetohydrodynamics. Incompressible effects explain the rapid evolution of turbulence in slow wind containing the heliospheric current sheet. The relative constancy of the spectrum of “inward propagating” fluctuations compared to the rapid decline in “outward” fluctuations results from incompressible spectral transfer combined with strong dissipation of the outward fluctuations. Secondary compressive effects account for nearly pressure-balanced structures and the density fluctuation levels.

PACS numbers: 96.60.Vg, 52.30.-q, 52.65.+z, 96.50.Bh

Observations of the solar wind have suggested that the dynamical evolution of the interplanetary magnetic field and plasma might be viewed as largely passive wave fields convecting from solar sources [1] or alternatively as actively evolving turbulence [2]. Recently [3], it has become clear that the latter interpretation generally holds, although significant questions remain concerning whether the dynamics can be successfully explained in the language of nearly incompressible magnetohydrodynamic (MHD) turbulence or whether strong compressive effects, arising from fully compressible turbulence or from convected compressive structures of solar origin, play an essential role. A number of recent observational papers [4–8] present evidence for the latter point of view; here we present simulations that provide a unified explanation for these observations entirely from the nearly incompressible MHD viewpoint.

The dynamical evolution of the magnetic and velocity fluctuations in the solar wind provides a unique opportunity for the study of MHD turbulence. The large spatial and temporal scales in the solar wind, combined with the highly super-Alfvénic speed of the flow, make possible observations of large, energy-containing structures on scales of fractions of an astronomical unit (AU) down to the dissipation range. Observations of the wind at different heliocentric distances give a time history of the turbulence. Power spectra of the fields, anisotropies in these spectra, and correlations between the variables evolve as the flow moves outward, and these changes are consistent with the evolution of the solar wind through a turbulent cascade [3].

Belcher and Davis [1] found that the fluctuations in the magnetic and velocity fields in the trailing edges of high-speed solar-wind streams could be interpreted as outward traveling Alfvén waves; elsewhere the fluctuations were less Alfvénic. More recently, Marsch *et al.* [9] showed that slow wind could also be highly Alfvénic, and Roberts *et al.* [10] showed that this was commonly the case far from solar minimum. We suggest here that the feature leading to these differences is that the slow wind at solar minimum contains the heliospheric current sheet; the lack of a magnetic-field component parallel to the velocity,

especially when near strong shear layers, allows the turbulent evolution to proceed rapidly. The incompressible MHD simulations described below also exhibit other characteristics of the spacecraft data [4–6] including the existence of a “background” spectrum [7], the rapid evolution of the initially outward propagating Alfvénic fluctuations toward this spectrum [8], and the seemingly “dissipationless” evolution [11] of the amplitude of the spectrum at higher wave numbers in the outer heliosphere. Compressible MHD simulations with the same initial conditions show very similar evolution but also include the development of nearly pressure-balanced structures and enhanced density fluctuations associated with the rapid evolution near current sheets, which are also features of the observations. While these simulations were carried out in two dimensions (2D), we believe that the mechanisms suggested here are likely to be operative in 3D [12]. These simulations thus offer a simple explanation of the observed radial evolution and stream structure of solar-wind fluctuations.

The incompressible spectral method code [13] and compressible pseudospectral code [14] used here resolve structures near the grid scale while still preserving ideal global invariants. The present results were obtained with fairly low resolution runs (64×64 modes) and mechanical and magnetic Reynolds numbers of 200. Higher resolution is only needed to determine details such as precise spectral slopes [15].

Among the conserved invariants are the total energy (per unit mass) $E = \frac{1}{2} \int d^2x (\mathbf{v}^2 + \mathbf{b}^2)$ and the cross helicity $H_c = \frac{1}{2} \int d^2x \mathbf{v} \cdot \mathbf{b}$ for a velocity \mathbf{v} and magnetic field \mathbf{b} in units of the Alfvén speed. In the compressible case, the conserved energy includes an internal energy term. We carry out much of the analysis using Elsässer variables, $\mathbf{z}^\pm = \mathbf{v} \pm \mathbf{b}$, which distinguish “outward (inward) traveling Alfvén waves” \mathbf{z}^+ (\mathbf{z}^-). The quotes indicate that what is primarily implied is the correlation between the magnetic and velocity fields; when a state which is neither purely \mathbf{z}^+ nor \mathbf{z}^- occurs, it could consist of mixtures of Alfvénic and non-Alfvénic fluctuations, and even with no mean field the correlations may still exist although they do not imply propagation. The degree of

Alfvénicity can be represented by the “reduced cross helicity” $\sigma_c = 2H_c/E$ so that purely outward propagating waves have $\sigma_c = +1$.

The initial conditions consisted in the first case of a relatively narrow “low-speed stream (LSS)” — a change of frame makes it “fast” — surrounded by high-speed streams (HSS) on either side (all in the x direction) with a current sheet embedded in the middle of the slow wind. The zero-momentum frame is used and we neglect the effects of weak spatial inhomogeneities at the scale of the simulation box. The magnetic and velocity shear layers are determined by the six lowest Fourier modes for the expansion of a square wave, and thus there are oscillations away from the major shears; these are physically reasonable and represent the irregularities always present within streams [16]. In incompressible 2D MHD a magnetic field transverse to the simulation plane has no effect on the dynamics and thus the observed fact that the magnitude of the magnetic field across the interplanetary current sheet is roughly constant can be maintained. Another simulation had the same stream structure as the first but contained a uniform applied magnetic field throughout the box, with no current sheets. In both cases a population of purely Alfvénic fluctuations with a fairly flat spectrum (modal spectral index -1) was added at wave numbers above those defining the shear layers, and a small random fluctuation (about 1% of the total energy) was added isotropically to modes with $|\mathbf{k}| \leq 6$ to initiate nonlinear couplings. The Alfvénic population models the observed fluctuations, but we assume that both slow and fast wind started out Alfvénic due to the condition of outward propagation at the critical point where the flow speed equals the Alfvén speed near $20R_S$ (≈ 0.1 AU). We show that departures from this “pure” state observed by spacecraft near and beyond 0.3 AU are consistent with dynamical evolution and do not require that static, low-cross-helicity structures convect from the Sun [4,7,17].

Figure 1 presents 1D energy spectra in terms of Elsässer variables in the incompressible case. The top panel shows that the dominant outward propagating fluctuations initially relax rapidly toward a steeper spectrum and then evolve more slowly (cf. the model of Tu [18]). We associate the time evolution in the simulation with radial evolution of the wind: $T=3$ is roughly equivalent to 1 AU. Initially the low- k fluctuations are non-Alfvénic, but the high- k fluctuations are purely Alfvénic as seen by the lack of z^- power at $T=0$. While the small-scale z^+ variations are rapidly dissipated, the z^- establishes and maintains a steady state. Shear-driven turbulence has nearly equal large-scale inputs to the cascade of both z^+ and z^- energies [15,19]. The z^- energy attains a steady state matched by dissipation, whereas the z^+ dissipation is greatly enhanced by the high power levels at high k . This behavior is observed in the inner heliosphere [7] with a background spectrum of z^- that is approached in time by z^+ . Subsequently, in the outer heliosphere, the spec-

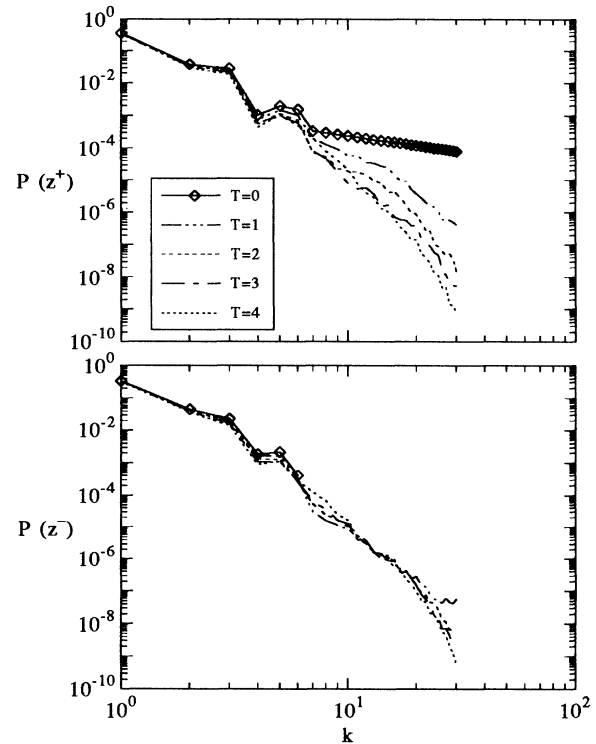


FIG. 1. Time evolution of the power spectra of the Elsässer variables z^+ and z^- for the incompressible run containing current sheets.

tra gradually evolve toward [10] each other, presumably with a slow cascade matched by slow dissipation, and this quasisteady state leads to an evolution of the amplitudes that is nearly that of dissipationless Alfvénic turbulence [11].

The background spectrum of z^- is observed to vary, and in particular there are increases in its level associated (at solar minimum) with low-speed wind. Figure 2 shows Elsässer spectra for a typical cut in x in the middle of the HSS of the simulation, and for a cut near the current sheet LSS. These spectra are one-dimensional power per wave number, similar to what would be found from spacecraft data. We see the characteristic “breathing” that was originally pointed out by Grappin, Mangeney, and Marsch [5], although the z^- increases somewhat more here than is observed. Spectra for a cut near the current sheet at the edge of the box, in the middle of the HSS, look like the LSS spectra shown here, indicating that proximity to the current sheet is the critical factor and not the speed of the wind or even the proximity of large shear layers.

The spatial structure of the fluctuations can be analyzed by filtering out all power with $|k_x|$ or $|k_y| < 8$, and then inverse transforming the resulting coefficients. At $T=1$ for the case with current sheets, σ_c derived from such a procedure deviates significantly from $+1$ at the location of the current sheets rather than where the vorticity is large. By contrast, without current sheets the strong

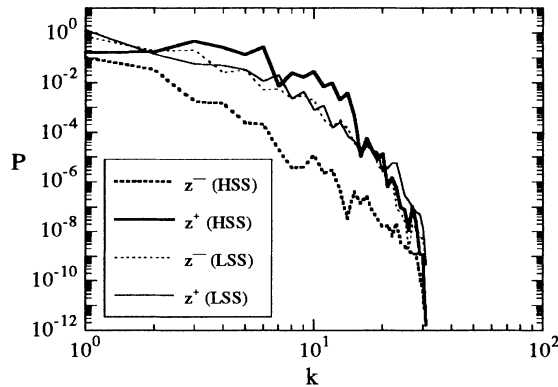


FIG. 2. Elsässer spectra for high- and low-speed streams taken from cuts along x in the simulation box.

shear layers are the dominant source of the evolution [15]. Figure 3 shows the spatial evolution of B_x , V_x , σ_c , and ω for the incompressible case with current sheets using plots as a function of y averaged over x . The top panel of the figure shows that the field and vorticity structure have been maintained on average, but that σ_c at high k (originally +1 everywhere) has been significantly decreased in the region of the current sheets near the edge and the middle of the box and especially so when the current sheet is near the strong velocity shear layers. This effect is observed in the solar wind. Even the low σ_c values in high-speed regions near points with no radial magnetic field are evident in Fig. 1 of Ref. [15]. By $T=4$ the cross helicity is low everywhere, on average, although a 2D spatial plot shows that there are both positive and negative regions that contribute. There has been no significant spreading of the current sheet region, considered as bounded by the vorticity layers, as would have been expected in a “spreading turbulent wake” picture [6].

The compressible simulation of the situation with the current sheet, with an initial turbulent sonic Mach number of 0.3 (typical of solar-wind values) and $\gamma = \frac{5}{3}$, yields nearly identical evolution of the “incompressible” quantities (σ_c, V_x, B_x), as shown in Fig. 4 for $T=2$. The new features are a persistent anticorrelation between the magnetic-field magnitude and the density ($r_{B,\rho}$), suggestive of nearly pressure-balanced “pseudosound,” and a density fluctuation that correlates well with the fluctuations in z^- . This correlation has been pointed out previously [4,5], associated with arguments that the appearance of high compression (measured, for example, by high $\delta\rho/\rho$, here approximately equal to $\delta\rho$ because $\rho \approx 1$) indicated the essential role of compression in understanding the plasma evolution. The present simulations indicate that the larger density fluctuations are probably primarily a by-product of the incompressible evolution [20].

The simulations also show essentially the correct behavior of the “Alfvén ratio” r_A between fluctuating kinetic and magnetic energy. The values of r_A remain near 1,

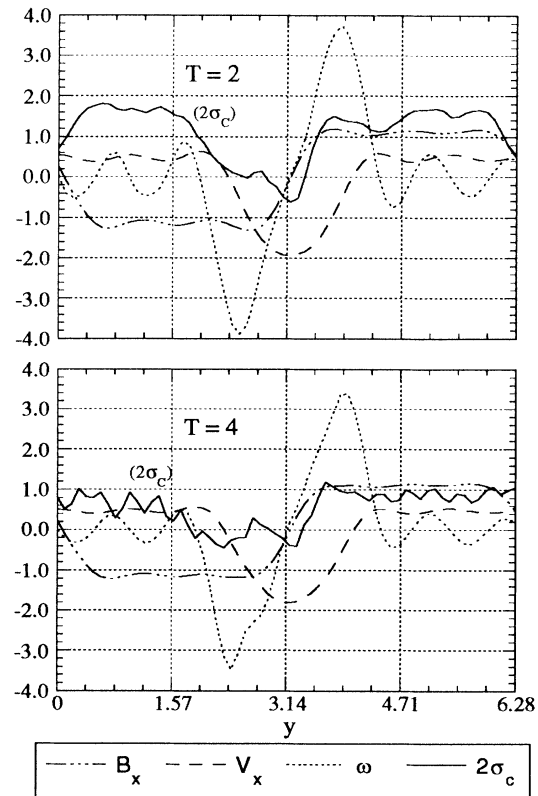


FIG. 3. Quantities averaged over x at $T=2$ and $T=4$ for the incompressible run with current sheets.

and although the mean value is in fact very close to 1 at $T=2$ (somewhat higher than the observed 0.5), the distribution of r_A values is strongly peaked near 0.5, and there are regions of lower r_A associated with low-cross-

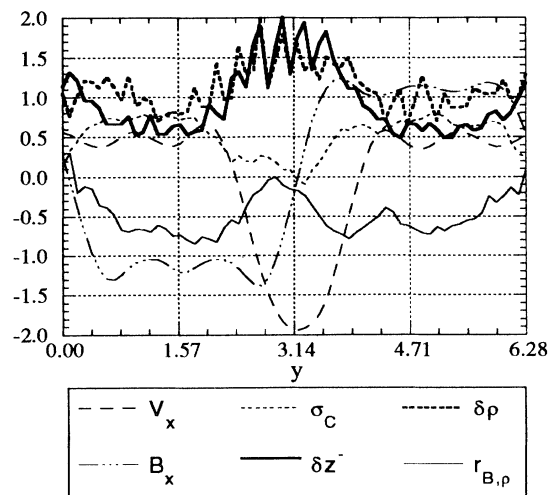


FIG. 4. Quantities averaged over x at $T=2$ for the compressible run with current sheets. The density and z^- fluctuations are normalized to twice their maximum values (0.042 and 0.075, respectively).

helicity regions such as were recently reported by Tu and Marsch [17]. While there is no simple association between r_A and σ_c in either the simulations or the observations, both quantities tend to have their lowest values in regions that are more strongly developed, and both tend to be near +1 in more purely Alfvénic regions, as expected.

We conclude that much of the evolution of interplanetary field fluctuations is accounted for by nonlinear incompressive MHD processes. The shear in the velocity field produced near the Sun leads to approximately equal injection of power in z^+ and z^- at large scales. Because z^- is initially small at high wave numbers, this injection leads to a spectrum that grows until it is balanced by dissipation; both injection and dissipation then remain at a relatively low, nearly constant level. The z^- spectrum thus is well developed, or “old” [6], very near the Sun. The injection of z^+ is inadequate to balance the rapid dissipation of the large high- k fluctuations, and thus the z^+ spectrum initially decreases rapidly. When the z^+ level is nearly equal to the z^- level the two spectra continue to evolve slowly toward each other with their overall amplitudes decreasing at nearly the rate they would if no spectral transfer were occurring.

This process is accelerated in the regions where the local mean field has a small component along the shear layer and especially, as for the heliospheric current sheet at solar minimum, when this occurs near strong shear layers. In the latter regions the rapid dissipation of the flat z^+ spectrum has already occurred by the time it is observed at 0.3 AU; thus the turbulence is “older” and the observed temperature evolution is nearly adiabatic [21]. By contrast, regions experiencing the rapid z^+ decay outside 0.3 AU have a slower than adiabatic temperature decrease because the dissipation heats the plasma. Broad slow-speed regions that do not contain a current sheet have properties similar to high-speed streams at solar minimum. Compressive effects are largely a result of the incompressive dynamics, as is to be expected in flows with low turbulent sonic Mach numbers.

This work was supported, in part, by the NASA Space Physics Theory Program at the Goddard Space Flight Center and NSF Grant No. ATM-8913627 at the Bartol Research Institute.

- [1] J. W. Belcher and L. Davis, *J. Geophys. Res.* **76**, 3534 (1971).
- [2] P. J. Coleman, *Astrophys. J.* **153**, 371 (1968); **153**, 1968 (1968).
- [3] D. A. Roberts and M. L. Goldstein, *Rev. Geophys., Suppl.*, 932 (1991); E. Marsch, in *Physics of the Inner Solar System II*, edited by R. Schwenn and E. Marsch (Springer, New York, 1991).
- [4] B. Bavassano and R. Bruno, *J. Geophys. Res.* **94**, 11977 (1989); R. Bruno and B. Bavassano, *J. Geophys. Res.* **96**, 7841 (1991).
- [5] R. Grappin, A. Mangeney, and E. Marsch, *J. Geophys. Res.* **95**, 8197 (1990).
- [6] R. Grappin, M. Velli, and A. Mangeney, *Ann. Geophys.* (to be published).
- [7] C.-Y. Tu and E. Marsch, *J. Geophys. Res.* **95**, 4337 (1990).
- [8] E. Marsch and C.-Y. Tu, *J. Geophys. Res.* **95**, 8211 (1990); **95**, 11945 (1990).
- [9] E. Marsch, K.-H. Mühlhäuser, H. Rosenbauer, R. Schwenn, and K. U. Denskat, *J. Geophys. Res.* **86**, 9199 (1981).
- [10] D. A. Roberts, L. W. Klein, M. L. Goldstein, and W. H. Matthaeus, *J. Geophys. Res.* **92**, 11021 (1987); D. A. Roberts, M. L. Goldstein, L. W. Klein, and W. H. Matthaeus, *J. Geophys. Res.* **92**, 12023 (1987).
- [11] D. A. Roberts, L. W. Klein, and M. L. Goldstein, *J. Geophys. Res.* **95**, 4203 (1990).
- [12] T. Stribling and W. H. Matthaeus, *Phys. Fluids B* **2**, 1979 (1990).
- [13] W. H. Matthaeus and S. Lamkin, *Phys. Fluids* **29**, 2513 (1986).
- [14] S. Ghosh and W. H. Matthaeus, *Phys. Fluids B* **2**, 1520 (1990).
- [15] D. A. Roberts, M. L. Goldstein, W. H. Matthaeus, and S. Ghosh, *J. Geophys. Res.* (to be published).
- [16] K. M. Thieme, E. Marsch, and R. Schwenn, *Ann. Geophys.* **8**, 713 (1990).
- [17] C.-Y. Tu and E. Marsch, *Ann. Geophys.* **9**, 319 (1991).
- [18] C.-Y. Tu, *J. Geophys. Res.* **93**, 7 (1988).
- [19] R. Grappin, A. Pouquet, and J. Léorat, *Astron. Astrophys.* **126**, 51, 1983.
- [20] D. Montgomery, M. Brown, and W. H. Matthaeus, *J. Geophys. Res.* **92**, 282 (1987); W. H. Matthaeus, L. W. Klein, S. Ghosh, and M. R. Brown, *J. Geophys. Res.* **96**, 5421 (1991).
- [21] J. W. Freeman, *Geophys. Res. Lett.* **15**, 88 (1988).